Rheological Characterization of the Gel Point in Polymer-Modified Asphalts

M. A. Vargas, O. Manero

Instituto de Investigaciones en Materiales, Universidad Nacional Autónoma de México, A.P. 70-360, México, D.F. 04510

ABSTRACT: In this work, the rheological characterization of the gel point in polymer-modified asphalts is carried out. The viscoelastic properties of polymer-modified asphalts, in which the polymer is styrene–ethylene butylene–styrene (SEBS) with grafted maleic anhydride (MAH), were measured as a function of MAH concentration. The crosslinking reaction that leads to gelation is characterized by power-law frequency-dependent loss and storage modulus (G'' and G'). The relaxation exponent n (a viscoelastic parameter related to the cluster size of the gel) and gel strength S (related to the mobility on the crosslinked chain segments) were determined. The value of the power-law exponents depends on the composition of polymer, ranging from 0.30 to 0.56, while the value of the rigidity modulus at the gelation point (S) increases with the amount of reactive groups of the modifier polymer. Both n and S are temperature-dependent in the blends. The blends containing gels present a coarse morphology, which is related to the rheological properties of the matrix and dispersed phase. © 2010 Wiley Periodicals, Inc. J Appl Polym Sci 119: 2422–2430, 2011

Key words: asphalt; functionalized polymers; gel point; power-law; relaxation exponent

INTRODUCTION

Asphalts are materials widely used in paved roads due to good adhesion with mineral solids, low cost, and adequate viscoelastic properties.[1–7] They are also used in the coating and adhesive industries. With the purpose to improve the mechanical and thermal properties of asphalt, a variety of polymers are used, among them functionalized polymers. Examples of reactive polymers of this sort are glycidyl methacrylate (GMA) with ester groups (methyl, ethyl or butyl), which are amply used as compatibilizers of various polymer blends, such as polyethylenes with polyamides or polyolefines with polyesters.[1,2]

Usually, a thermoplastic copolymer is functionalized with reactive compounds, e.g., fatty dialkyl amide, to induce a reaction with asphalt. Examples of some functionalized polymers used to modify asphalt are SEBS-*g*-MAH and Zn-sulfonated-SBS.[1]

In particular, styrene-*b*-(ethylene-1-butene)-*b*-styrene "SEBS" copolymers functionalized with maleic anhydride (MAH), (SEBS-*g*-MAH) have been used as compatibilizers of immiscible polymer blends.

These copolymers react with hot asphalt to form a polymer-linked-asphalt system with improved properties.[1] For reactive compatibilization to occur in polymer blends, some conditions have to be met: (1) the presence of reactive functional groups capable of reacting at the interface of the polymers, (2) the reaction should occur within the residence time of the processing and curing processes, and (3) the bonds formed should be stable to any further processing.[1,2,4] This chemical bond impedes phase separation among the ingredients of the blend when they are subjected to extreme storage conditions.

The asphalt modification by reactive polymers (GMA, SEBS-*g*-MAH), requires that the amount of polymer is chosen carefully because an excessive quantity leads to the formation of insoluble and infusible asphalt gels.[2,8] For this reason, reactive polymers are added in quantities usually ranging from 1.5 to 2.5 wt %. The chemical bonds formed among polymer chains and asphalt molecules lead to the generation of a network, which should be kept below the "chemical" gel point; this means that the reaction must be stopped when the crosslinking polymer (consisting of a distribution of clusters) swelled by asphalt may still be dissolved in solvents.

Unfortunately, due to the extremely complex chemical composition of asphalts, it is difficult to determine the identity of chemical bonds formed during the curing process, and no clear experimental data have been reported to this regard.[2]

When the asphalt is mixed with SEBS-MAH and following processing and curing processes, it is likely that the MAH groups of SEBS react with carboxylic groups of the asphaltenes, thus forming ester links and anhydrides. Moreover, if the asphaltene molecule, or micelle, contains more than one carboxylic group, a chemical crosslinked network may theoretically be formed.[1,2] Asphaltenes may contain other reactive groups such as hydroxyl, amines, and so on, which induce reactions leading to physical or chemical crosslinking.[1–3]

The gelation point of a crosslinking polymer is an important parameter,[9,10] whose evaluation provides important information on the performance of materials, and this is accomplished by means of rheological and thermal testing to assess the processing and storage conditions. In particular, the evolution of the rheological properties in the curing system provides valuable data to determine the gelation properties of the system. The linear viscoelastic properties are sensitive enough to the network formation and to the presence of a gelation point.[9,11–13] This can be defined as the point where a tridimensional network of flexible, yet crosslinking polymer chains, forms. Rheologically, the gelation point marks the transition from a viscoelastic liquid into a nearly Hookean viscoelastic solid,[10] depending on time, temperature, concentration and polymer properties.[9,11,13,14] In this transition, the zero shear-rate viscosity and relaxation time diverge,[11,13] under conditions evolving far from thermodynamic equilibrium. Attention is given in this work to the gelation point determination through thermal stability tests (curing process).[15,16]

Background

Various models have been proposed to analyze the formation and properties of gelation systems[9,11,13] but in most complex systems these are still standing problems. Scaling theories intended to describe the sol–gel transition[11] suggest power-law behavior of the rheological and other physical properties.

Winter and Chambon found that at the gelation point the rheological behavior can be described by power-law frequency-dependent storage and loss modulus[10–12]:

$$G'(\omega) = S\Gamma(1-n)\cos(n\Pi/2)\omega^n \quad (1)$$

$$G''(\omega) = S\Gamma(1-n)\sin(n\Pi/2)\omega^n \quad (2)$$

$$0 < n < 1 \quad (3)$$

$$0 < \omega < 1/\lambda_0 \quad (4)$$

where n is the power-law exponent, S is the rigidity modulus at the gelation point, Γ is the gamma function, and λ_0 is the characteristic time of the prepolymer and marks the transition into a glassy state.[12]

The exponent n depends on composition and crosslinking degree according to data from polymeric networks[9,14] and lies in the interval $0 < n < 1$. However, some theories suggest that the power-law exponent may be independent of molecular structure.[17] On the other hand, the gel rigidity modulus S [eqs. (1) and (2)] is given by:[12,13,17]

$$S = G_0\lambda_0^n \quad (5)$$

where G_0 is the plateau modulus. For crosslinked materials, the rigidity modulus approaches G_e. $G_0\lambda_0$ is equal to the shear viscosity of the prepolymer (η_0).[12,13]

The gel strength (S) depends on the flexibility of molecular chains and crosslinks density at the gel point. The relaxation exponent n is related to the geometry of clusters existing at the gel point.[18] In general, a lower value of n implies formation of a more highly elastic gel, while the same value of n means equivalent viscoelasticity.[19]

At the gelation point, the loss and storage modulus follow parallel curves according to:

$$G'(\omega) \propto G''(\omega) \propto \omega^n \quad (6)$$

Consequently, the loss tangent (tan δ) is independent of frequency (ω), i.e.,

$$\tan\delta = G''/G' = \tan(n\Pi/2) \quad (7)$$

The region where the loss tangent is independent of frequency in the vicinity of the gelation point has been used as a criterion to identify crosslinking.[9,11,12,17,20–23] These values of the loss tangent were taken in a range of frequency when plotted with time may converge to the gelation time t_{gel}. This criterion has been proved to be very useful since the key variable for describing the gelation point becomes independent of frequency and diverges at this point. Results are valid for a gelation point determined as a function of temperature and time, but it has not been reported as a function of concentration.[11] Notwithstanding, the power-law exponent n is not constant nor universal, but a function of the specific properties and dynamics of the system, according to reported experimental data.[9,11,12,17] Some theories on gelation properties of materials describe this process as increasing molecular disorder.[20] Percolation theories indicate that $G' = G'' \approx \omega^n$ with $n = 2/3$, while several reports have found a value near 0.8 in crosslinked PVC, 0.2 for vulcanized PE and near 0.2 for crystalline polypropylene.[11,20]

In this work, the sol–gel transition (gelation point) of a system constituted by asphalt and reactive polymers is characterized by rheometric measurements, solubility test, thermogravimetric analysis (TGA),

and fluorescent microscopy. The resulting structure of the crosslinked polymers depends on the reactive group concentration (MAH), temperature and concentration of the modified polymer. The effect that the concentration of reactive groups of the modified polymer has on the formation of gelled or crosslinked systems after the curing process is analyzed here for modified asphalts.

EXPERIMENTAL

Sample preparation

The samples of modified asphalts were obtained after high-temperature storage tests[24] using asphalt (with 80/20 wt % maltene/asphaltene composition) mixed with SEBS polymers grafted with specific amounts of MAH (SEBS-MAH24, SEBS-MAH34, SEBS-MAH54, and SEBS-MAH74).[24-26] The polymer content in the asphalt is 4 wt %. The properties of modifier polymers are shown elsewhere.[24] SEBS-MAH24, 34, 54 and 74 means 4 wt. % polymer and 2,3,5 and 7 wt. % MAH

Gel content testing

The gel point was determined experimentally as the point at which soluble polymers were obtained but the mixture was not soluble in THF.[27-29] THF was used at room temperature. Each sample was immersed in excess of THF, and the solvent was replaced every day over a period of 3 weeks until no further extractable polymer can be detected. The resulting gels were filtered and washed with THF. The procedure was repeated five times to fully remove the soluble fraction. The gels were dried preserving constant weight. The weight fraction of gel was calculated as[27-29]:

$$Gel = \frac{m_{gel}}{m_{blend}} \quad (8)$$

where m_{gel} and m_{blend} are the dry gel weight and the weight of the blend, respectively.

Fluorescence microscopy

Polymer distribution in the PMA macro-phase after the curing process was observed by fluorescence microscopy using a Carl-Zeiss KS 300 microscope at ambient temperature with a wavelength of 390–450 nm at 20X. Micrographs were taken with a MC100 camera equipped with an automatic counter. The polymer rich phase appears white while the asphalt rich phase is dark. Time, temperature, and concentration-dependent changes of the rheological properties of the blends during the curing process also affect strongly the morphology and conse-

quently the characteristics of polymer. Specifically, the increase in viscosity of the polymer that undergoes crosslinking and the decrease in viscosity of the one experiencing degradation influence profoundly the size and shape of the dispersed phase.

Thermogravimetric analysis

TGA of the blends was carried out in a TA-Instruments SDT Q600 system. TGA tests used alumina crucibles, where samples (5–10 mg weight) were placed on the balance with rising temperature from 25 to 400°C at a heating rate of 10°C/min. The mass of the sample pan was continuously monitored as a function of temperature. TGA experiments were carried out under nitrogen environment using a flow rate 100 mL/min to avoid thermo-oxidative degradation. Decomposition temperature (T_d) in nitrogen was taken as the temperature corresponding to 5 and 10% weight loss, respectively.

Rheological experiments

Measurements of the loss and storage modulus as functions of frequency of the segregated samples of the polymer-modified asphalts were performed in an AR-1000 TA controlled stress rheometer using a parallel plate fixture of 2-cm diameter and 1-mm gap. The linear viscoelastic region was found from measurements of the moduli versus % strain at fixed frequency. A temperature sweep from −5 to 120°C at 2°C/min and a frequency sweep from 0.1 to 100 rad/s at various temperatures (−5, 15, 20, 40, 60, 75, and 100°C) were carried out.

RESULTS AND DISCUSSION

Gel fraction (wt %)

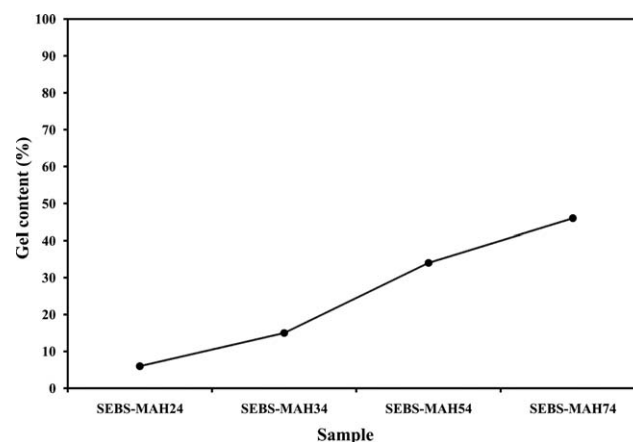The gel content (%) is shown in Figure 1 as a function of the amount of MAH grafted. Gel increases

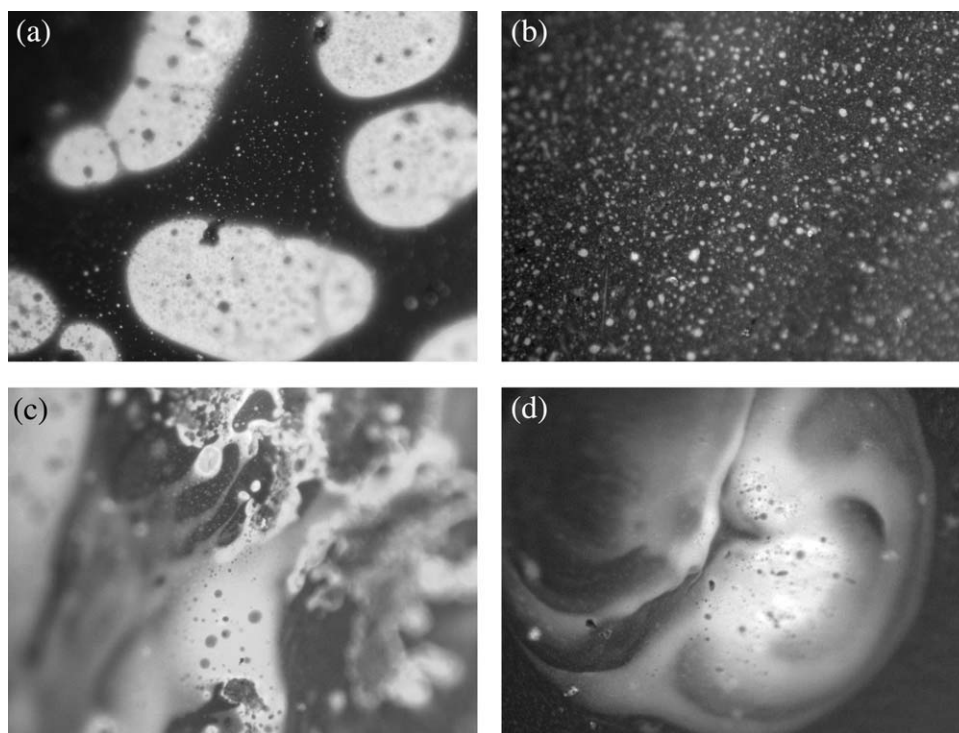**Figure 1** Gel content (%) as a function of MAH amount of blends.

Figure 2 Fluorescence microscopy of blends after the curing process: (a) asphalt/SEBS-MAH24, (b) asphalt/SEBS-MAH34, (c) asphalt/SEBS-MAH54, and (d) asphalt/SEBS-MAH74.

with the amount of MAH up to the highest value corresponding to the asphalt/SEBS-MAH74 sample.

Fluorescence microscopy

Figure 2 shows the morphology of the blends after the curing process. The morphological analysis demonstrates that the asphalt/SEBS-MAH24 blend is unstable under high temperature storage conditions, but apparently gel is not formed [Fig. 2(a)]. This picture agrees with a lower compatibility and weak interfacial adhesion of the polymer. Figure 2(b) shows the micrographs of asphalt/SEBS-MAH34, exhibiting a shadowy continuous phase, in which small light spots of comparable dimensions are quite homogeneously distributed. Considering the chemical nature of the bonds that are generated between polymer chains and/or polymer chains and asphalt

molecules, reactive polymers can be used only if the forming network is kept below "chemical" gel point.

The morphological analysis of asphalt/SEBS-MAH54 suggest that MAH content of 5% is probably the upper limit for gel appearance, as demonstrated by micro-scale morphology [Fig. 2(c)]. For a curing time of 3 days at 180°C, the accumulated particle size of polymer increased. Prior to the gel point, the crosslinking polymer consists of a distribution of clusters; but beyond the gel point, it is swelled by asphalt but unable to melt or dissolve in solvents. The asphalt modified by SEBS-MAH74 [Fig. 2(d)] leads to a system with irregular particle shapes and with no clear dispersed phase.

Thermogravimetric analysis

The degradation temperature of blends was determined using TGA. Table I discloses the wt % loss of

TABLE I
Effect of Grafted MAH Content on Weight Loss at Various Temperatures and Decomposition Temperatures

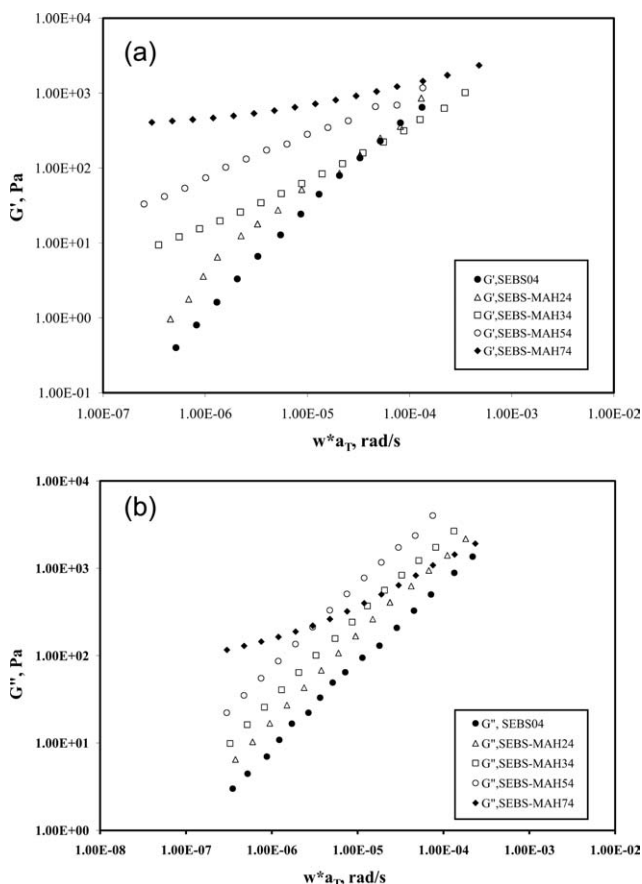| Sample	Weight loss (%) at temperature				$T_{5\%}$ (°C)	$T_{10\%}$ (°C)
	250°C	300°C	350°C	400°C		
SEBS-MAH24	2.0	4.6	12.0	25	305	330
SEBS-MAH34	1.0	2.7	8.7	15	320	360
SEBS-MAH54	0.3	1.0	4.3	10	355	400
SEBS-MAH74	0.1	0.5	1.2	8	362	–

Figure 3 Viscoelastic properties of blends as a function of MAH content: (a) elastic modulus and (b) loss modulus.

the sample at four selected temperatures (250, 300, 350, and 400°C). As the wt % of grafted MAH increases, a gradual decrease in weight loss can be noticed (at 250 and 400°C) indicating improvement in thermal stability. Asphalt/SEBS-MAH74 possesses better thermal stability with no significant weight loss compared with the other blends. The decomposition temperature of the blends for 5% weight loss ($T_{5\%}$) and weight loss ($T_{10\%}$) increases with the increasing MAH content, manifesting better thermal stability.[30,31]

Viscoelastic properties of blends

The storage and loss modulus as a function of frequency measured after high-temperature storage tests are shown in Figure 3. The blends asphalt/SEBS04 and asphalt/SEBS-MAH24 do not contain gel and they are in the prepolymer stage since $G'' > G'$. When G'' is close to G', the system is in the sol–gel transition zone (asphalt/SEBS-MAH34 and asphalt/SEBS-MAH54). Beyond this critical point the moduli grow and G' and G'' have comparable values. However, G' increases much faster than G'' as the MAH content rises, exhibiting the typical evolu-

tion of a gelation process.[32] At low frequencies, both shear moduli are parallel to each other over one decade indicating that the gel point was reached.[33] Past the gel point, the storage modulus G' becomes larger than G'' and the system now behaves as a viscoelastic solid (asphalt/SEBS-MAH74) along the post-gel regime.[13,18,34] It is apparent that G' is very sensitive to the MAH content, as shown in Figure 3(a).

Figure 4 shows the Black plots of the blends. Only the asphalt with SEBS04 and SEBS24 fulfill superposition over the whole temperature range (materials without gel content). Upon increasing the reactive groups of the modifier polymer with appreciable gel formation, blends do not follow superposition, in addition to show predominant elastic behavior.[12,35–38]

Determination of the gelation point

At the gelation point, the moduli are expected to scale with frequency as $G' \sim G'' \sim \omega^n$. In fact, Winter et al.[10–12,39] reported power-law behavior of the shear modulus over a wide range of frequencies in systems with permanent gelation. Such generality has been criticized, since a general trend is a strong assumption that neglects entanglement effects. Other systems present rather low gel concentrations.[40]

In this work, the "apparent" power-law exponent n was determined by three methods:[22,41] (1) by considering the region where the two moduli are parallel (same n_{slope}); (2) by determining the intersection of tan δ curves along the frequency window (n_{tan}); and (3) by using eqs. (1) and (2);.

The power-law exponent $n = n_{slope}$ of the moduli was evaluated from the master curves of each material. The gelation criterion consistent with same power-law index of the moduli along a wide frequency range can be ascribed to a restricted relaxation as the liquid–solid transition evolves. In this perspective, the asphalt/SEBS-MAH24 blend does not present gelation characteristics since the slopes
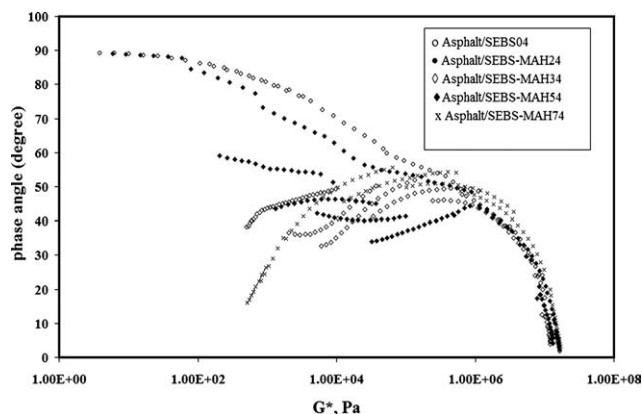

Figure 4 Black diagram. Phase angle versus complex modulus of the blends.

TABLE II
Slopes of G' and G'' at Small and High Frequencies

Sample	$(dG'/d\omega)_{\omega \to 0}$	$(dG''/d\omega)_{\omega \to 0}$	ω_c (rad/s)	$(dG'/d\omega)_{\omega \to \infty}$	$(dG''/d\omega)_{\omega \to \infty}$
SEBS-MAH24	1.50	1.0			
SEBS-MAH34	0.67	0.80	3.5×10^{-5}	0.38	0.38
SEBS-MAH54	0.50	0.60	6.3×10^{-4}	0.52	0.52
SEBS-MAH74	0.20	0.40	1.1×10^{-3}	0.50	0.50

are not equal, reflecting that the concentration of reactive groups is sufficiently low (Table II).

In the master curves of the gelled systems, i.e., asphalt/SEBS-MAH34, asphalt/SEBS-MAH54, and asphalt/SEBS-MAH74, it is possible to distinguish two regions: at low frequency, the limiting slopes present a departure from Maxwell behavior ($G' \propto \omega^2$, $G'' \propto \omega$ as $\omega \to 0$), whose values are disclosed in Table II, while at intermediate frequency ($5.75 \times 10^{-5} - 1.9 \times 10^2$ rad/s) the loss and storage modulus converge and show same slope with frequency, as disclosed in columns 5 and 6 of Table II. Here, the smallest slope is measured ($\omega^{n=0.38}$) corresponding to the asphalt/SEBS-MAH34 blend, while in asphalt/SEBS-MAH54 and asphalt/SEBS-MAH74 blends, the dependence for both blends follows the power law $\omega^{n=0.5}$, showing independence of the reactive groups concentration. This behavior is due to the fact that the power-law exponent increases with the amount of reactive groups, up to a limiting amount or saturation of these groups, where the exponent becomes independent of their concentration. G' and G'' are nearly parallel approaching a plateau (from 10^{-7} to 10^{-5}) in the low frequency range, consistent with the results reported by Nijenhuis and Winter.[39] Notwithstanding, the storage modulus at low frequency of the asphalt/SEBS-MAH74 blend is almost 3 decades larger than that of the asphalt/SEBS-MAH24 (not gelled) blend.

Since the gelation variable (tan δ) becomes independent of frequency and converges to a single point, the gelation point is then determined by plotting the loss tangent in a frequency range as a function of the variable that governs the crosslinking process (time, temperature or concentration). In the present case, this variable is the concentration of reactive groups in the modifying polymer.[11]

In Figure 5, the loss tangent of the four samples converges to a point with magnitude of 1.13 and frequency of 5×10^{-3} rad/s (gelation point). The power-law exponent (0.54) is calculated from eq. (7). This value is near that of the slopes at intermediate frequency of G' and G'' (Table II) for asphalt/SEBS-MAH54 and asphalt/SEBS-MAH74. In the pregel regime, the loss tangent decreases with increasing frequency, as in viscoelastic liquids (asphalt/SEBS-MAH24 blend), approaching a constant in the vicinity of the gelation point, indicating a predominant elastic behavior. This trend is observed in the

asphalt/SEBS-MAH34, asphalt/SEBS-MAH54, and asphalt/SEBS-MAH74 blends. Tan δ (ω) of asphalt/SEBS-MAH34, asphalt/SEBS-MAH54, and asphalt/SEBS-MAH74 is independent of frequency and samples behave as critical gels (asphalt/SEBS-MAH34 and asphalt/SEBS-MAH54) and postgel (asphalt/SEBS-MAH74). This indicates that network clusters with high molecular weight are formed. Furthermore, near the gel point the frequency dependence of $G'(\omega)$ and $G''(\omega)$ can also be approximated by power laws, though, in a limited region. The exponents for $G'(\omega)$ and $G''(\omega)$ differ each other and they are dependent on the departure from the gel point; in this case asphalt/SEBS-MAH34 is near the gel point.

Figure 6 depicts the loss tangent as a function of MAH content in the polymer for various angular frequencies (0.1, 0.4, 1, 4, 10, 30, and 100 rad/s) at 100°C. A crossing point in the SEBS-MAH34 blend is observed. It is likely that at this concentration the gelation process starts, and thereafter, all curves converge to the value of the SEBS-MAH54 blend, namely, the critical concentration for gelation (C_g).

Values of n obtained from eqs. (1) and (2) provide a more accurate determination of the gel point. The exponents of the moduli, n_1 and n_2 for the blends are disclosed in Table III. Asphalt/SEBS-MAH34 presents different values for n_1 and n_2 as compared with the slope method (n_{slope}) in all frequency range. This effect can be traced to the small amount of gel formed. For the asphalt/SEBS-MAH54 blend, $n_1 =$
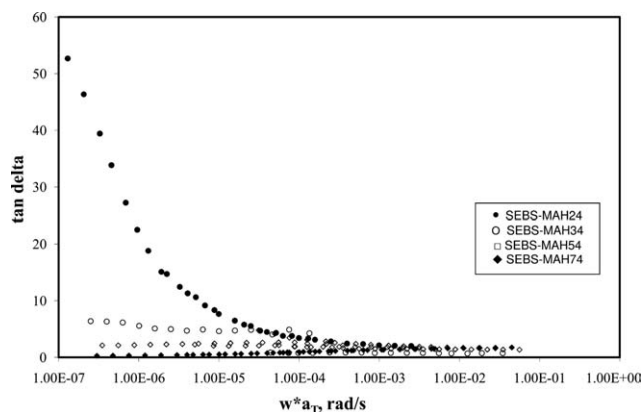

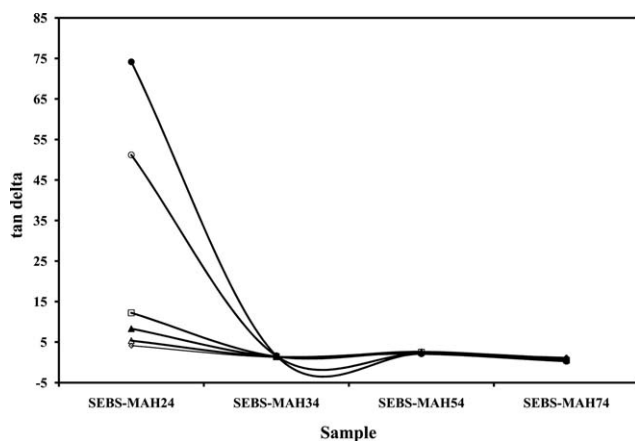**Figure 5** Loss tangent (tan δ) as a function of MAH content of the blends.

Figure 6 Loss tangent (tan δ) as a function of MAH content in the modifier polymer for various angular frequencies (0.1, 0.4, 1, 4, 10, 30, and 100 rad/s) at 100°C.

$n_2 = 0.5$ along the entire range of frequencies ($3.5 \times 10^{-7} - 1.9 \times 10^2$ rad/s).

For the asphalt/SEBS-MAH74 blend, values of n_1 and n_2 at low frequencies ($3 \times 10^{-7} - 2.52 \times 10^{-5}$) are $n_1 = 0.5$, $n_2 = 0.3$; $n_1 = 0.3$, $n_2 = 0.56$; and $n_1 = n_2 = 0.3$. At intermediate frequencies ($5.75 \times 10^{-5} - 1.9 \times 10^2$ rad/s) values are $n_1 = n_2 = 0.5$, while at high frequencies ($3 \times 10^2 - 1.87 \times 10^3$) they diminish, i.e., $n_1 = n_2 = 0.40$. On this basis, for this material, the power-law exponents of the dynamic moduli are affected by temperature.

Although the three approaches give different values of n, nevertheless the trend appears to be the same at intermediate frequencies independently of the method used for materials with a critical gel point. Values of n are reported in Table III.

The percolation theory predicts a power law exponent of $n = 0.67$ in the limit of Rouse dynamics (considering a model without hydrodynamics interactions), while simulations of the percolation theory, using an analogy of gelation to resistor-superconductor networks, gave $n = 0.73$. Finally, according to the mean field theory, n is equal to 1.[22]

However, it is now well established by several experimental studies that there in no such universal value for n, since it is actually dependent on various parameters, like polymer concentration, molecular weight and pregel history. Furthermore, in the presence of an excess of crosslinker, n assumes values smaller than those predicted by the mentioned theories.

Experimental results indicate that the gelation process is rather complex, and hence theoretical models aim to relate the dynamic exponent n with information about the molecular structure at the gel point. It is suggested that this structure may be represented by a fractal dimension d_f, which is defined by $R^{df} \sim M$, where R is the radius of gyration and M the mass of a molecular cluster. The fractal dimension measures the degree of packing of the structure; lower fractal dimension indicate a more open system, while higher fractal dimensions indicate a more packed system.[22,42] It means that for a particle aggregate having a lower fractal dimension, the molecular weight grows slower with radius that another aggregate having a higher fractal dimension.

All the critical gels from stoichiometrically balanced mixtures should have similar network structures. Main differences originating from variations in the strand length may enhance the excluded volume effect. In the case that the excluded volume is fully screened (reasonable assumption in the present work considering the relatively high polymer concentration), the following expression is suggested for polydisperse systems:[11,12–14,17,20–22,41–49]

$$n = \frac{d(d + 2 - 2d_f)}{2(d + 2 - d_f)} \tag{9}$$

where d is the space dimension, which in this case is 3.[12,14,17,22,44–49] In the framework of eq. (9), all values of the scaling exponent n are possible for a fractal in the physically realizable domain $1 \leq d_f \leq 3$. The relaxation exponent can be related to the conectivity properties of the incipient gel and it can give the fractal dimension at the gel point.

On the basis of eq. (9), values of d_f for each gel system lie in the range 1.73–2.1 for n_1 and 1.73–1.96 for n_2 (Table IV). According to eq. (9), a fractal dimension of 1.82 is obtained for asphalt/SEBS-MAH34 and asphalt/SEBS-MAH54. The same fractal dimensions suggest that the crosslinked structures produced at the gel point are similar for both systems and they are "open" structures. Values of n for asphalt/SEBS-

TABLE III
Comparison of the Gel Point Obtained by Three Different Methods

Sample	n_{1slope} $\omega \rightarrow 0$	n_{2slope} $\omega \rightarrow 0$	n_{1slope} $\omega \rightarrow \infty$	n_{2slope} $\omega \rightarrow \infty$	n_{tan}	eqs. (1) and (2)			
						n_1 $\omega \rightarrow 0$	n_2 $\omega \rightarrow 0$	n_1 $\omega \rightarrow \infty$	n_2 $\omega \rightarrow \infty$
SEBS-MAH34	0.67	0.80	0.38	0.38	0.54	0.5	0.5	0.5	0.5
SEBS-MAH54	0.50	0.60	0.52	0.52	0.54	0.5	0.5	0.5	0.5
SEBS-MAH74	0.20	0.40	0.50	0.50	0.54	0.5	0.3	0.4	0.4
						0.3	0.56	–	–
						0.3	0.3	–	–

TABLE IV
Values of d_f for Each Blend at Low and Intermediate Frequencies

Blend	d_f (n_1) $\omega \to 0$	d_f (n_2) $\omega \to 0$	d_f ($n_1 = n_2$) $\omega \to \infty$
SEBS-MAH34	1.82	1.82	1.82
SEBS-MAH54	1.82	1.82	1.82
SEBS-MAH74	2.10	1.73	1.96

MAH74 indicate that the fractal dimension decreases from 2.1 to 1.96 as temperature increases (from low frequencies to intermediate frequencies). This tend in d_f may suggest that the gel network becomes more "open" as temperature increases.[22]

Figure 7 shows the rigidity modulus at the gelation point (S) calculated from eq. (5) and $n = 0.5$ for intermediate frequencies. The rigidity modulus S increases with the MAH content of the polymer. Elsewhere,[11] it has been reported that for a constant n, the crosslink density of a strong gel leads to increasing S. Equation (5) illustrates that the gelation stress S is defined in terms of a critical gelation index, since this exponent determines the critical rate of relaxation at the gelation point.[11] S is a function of a short relaxation time λ_0 and modulus G_0, both are characteristic functions of the prepolymer. Reports have shown that S is sensitive to changes in the branching length. When the branches contract as the polymer concentration increases, the crosslink density augments, resulting in a strong gel with high S.[11,14] The rheological parameters of the critical gel (asphalt/SEBS-MAH54), are $S = 8.70 \times 10^5$ Pa s$^{0.50}$ and $n = 0.50$.

The gel strength parameter S as a function of temperature was determined from eqs. (1) and (2) and plotted in Figure 8. The gel stiffness decreases with increasing temperature. If the reaction mechanism would not change throughout the temperature range, G_0 should remain constant with increasing
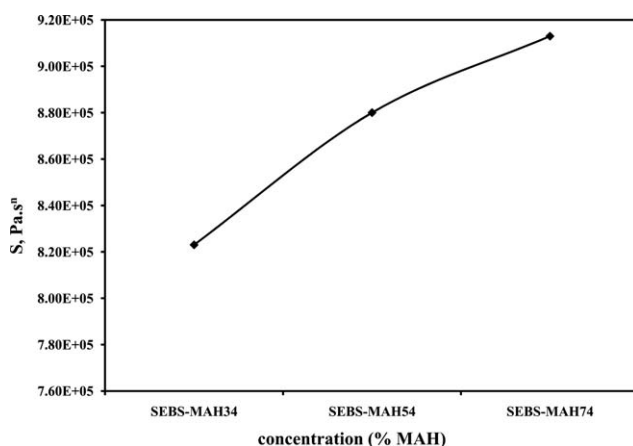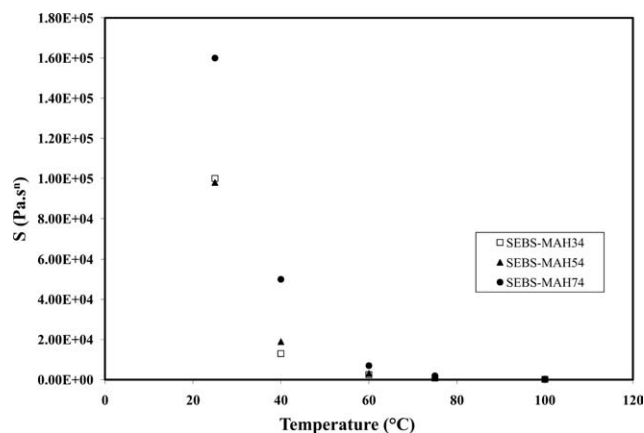

Figure 8 Gel strength parameter S [calculated from eqs. (3) and (4)] as a function of temperature.

temperature. Since η_0 (T) decreases with increasing temperature, then $S(T)$ decreases, as observed in the data analysis. Although no sound theoretical interpretation for S exists, it is believed that gel strength reflects the mobility of chain segments at the gel point. With increasing temperature, the gel strength S decreases due to enhanced chain mobility. Different cluster sizes at different temperatures may also contribute to decreasing S.[7,38,41,50–53]

CONCLUSION

The rheological properties of gelling systems were studied as a function of the degree of crosslinking. It was found that stable mixtures can be obtained if the MAH content is maintained below 5 wt %, while higher MAH content leads to gel formation during the curing process. The blends asphalt/SEBS04 and asphalt/SEBS-MAH24 do not contain gel, since these blends are in the prepolymer stage, while that asphalt/SEBS-MAH34 and asphalt/SEBS-MAH54 are in the sol–gel transition zone. In particular, asphalt/SEBS-MAH54 is the blend where critical gels are generated.

Past the gel point, the storage modulus G' becomes larger than G'', and the system behaves as a viscoelastic solid such as asphalt/SEBS-MAH74 along the postgel regime. Asphalt/SEBS-MAH54 and asphalt/SEBS-MAH74 display high thermal stability and high decomposition temperature.

The morphological analysis of asphalt/SEBS-MAH54 suggests that MAH content of 5 wt % is the upper limit for the gel point, as demonstrated by micro-scale morphology alteration, while the modified asphalt SEBS-MAH74 presents a "critical" condition, i.e., polymer particles form aggregates.

Determinations of the gel concentration, the gel stiffness S and the relaxation exponent n, were carried out by applying the Winter-Chambon criterion

Figure 7 The gel strength parameter S as a function of MAH content.

at the gel point. Here, the loss and storage modulus present power-law behavior with frequency. The critical exponent, n, was evaluated using three methods, namely, (1) G' and G'' become parallel in master curves (asphalt/SEBS-MAH34, asphalt/SEBS-MAH54 and asphalt/SEBS-MAH74), (2) tan δ becomes frequency-independent, and (3) using eqs. (1) and (2). The three approaches render similar values at intermediate frequencies for asphalt/SEBS-MAH54, while for asphalt/SEBS-MAH34 different values for n were obtained using the three methods along the full frequency range. This is likely an effect of the low amount of gel generated in this system. For asphalt/SEBS-MAH74, the exponent is dependent on temperature. The fractal dimensions, calculated assuming that the excluded volume effect is fully screened is indicative of a network that becomes more open as temperature increases for asphalt/SEBS-MAH74. Asphalt/SEBS-MAH34 and asphalt/SEBS-MAH54 present same fractal dimensions, suggesting that the crosslinked structures produced at the gel point are similar for both systems and they are "open" structures. The rigidity modulus (S) at the gelation point varies linearly with reactive group concentration (MAH) and reflects the mobility of chain segments. It was found to decrease with increasing temperature.

References

1. Becker, Y.; Mendez, M. P.; Rodriguez, Y. Visión Tecnologica 2001, 9, 39.
2. Polacco, G.; Stastna, J.; Biondi, D.; Antonelli, F.; Vlachovicova, Z.; Zanzotto, L. J Colloid Interface Sci 2004, 280, 366.
3. Becker, Y.; Muller, A. J.; Rodriguez, Y. J Appl Polym Sci 2003, 90, 1772.
4. Polacco, G.; Stastna, J.; Biondi, D.; Zanzotto, L. Curr Opin Colloid Interface Sci 2006, 11, 230.
5. Polacco, G.; Muscente, A.; Biondi, D.; Santini, S. Eur Polym J 2006, 42, 1113.
6. Wang, Q.; Liao, M.; Wang, Y.; Ren, Y. J Appl Polym Sci 2007, 8, 8.
7. Ait-Kadi, A.; Brahimi, B.; Mousmina, B. Polym Eng Sci 1996, 36, 1724.
8. Polacco, G.; Stastna, J.; Vlachovicova, Z.; Biondi, D.; Zanzotto, L. Polym Eng Sci 2004, 44, 2185.
9. Commereuc, S.; Bonhomme, S.; Verney, V.; Lacoste, J. Polymer 2000, 41, 917.
10. Lairez, D.; Adam, M.; Emery, J. R.; Durand, D. Macromolecules 1992, 25, 286.
11. Li, L.; Aoki, Y. Macromolecules 1997, 30, 7835.
12. Chiou, B. S.; English, R. J.; Khan, S. A. Macromolecules 1996, 29, 5368.
13. Eloundou, J. P.; Feve, M.; Gerard, J. F.; Harran, D.; Pascault, J. P. Macromolecules 1996, 29, 6907.
14. Kjoniksen, A. L.; Nyström, B. Macromolecules 1996, 29, 5215.
15. Horst, R. H.; Winter, H. H. Macromolecules 2000, 33, 7538.
16. Boey, F. Y. C.; Qiang, W. J Appl Polym Sci 2000, 76, 1248.
17. Izuka, A.; Winter, H. H. Macromolecules 1992, 25, 2422.
18. Hu, X.; Fan, J.; Yue, C. Y. J Appl Polym Sci 2001, 80, 2437.
19. Semsarzadeh, M. A.; Barikani, S. M. Macromol Symp 2006, 239, 245.
20. Scanlan, J. C.; Winter, H. Macromolecules 1991, 24, 47.
21. Rudé, E.; Llorents, J. J Non Cryst Solids 2006, 352, 2220.
22. Sandolo, C.; Matricardi, P.; Alhaique, F.; Coviello, T. Food Hydrocolloids 2008, 23, 210.
23. Nuñez, M. C.; Tecante, A. Carbohydr Polym 2007, 69, 763.
24. Vargas, M. A.; López, N. N.; Cruz, M. J.; Calderas, F.; Manero, O. Rubber Chem Technol 2009, 82, 244.
25. Passaglia, E.; Ghetti, S.; Picchioni, F.; Ruggeri, G. Polymer 2000, 41, 4389.
26. Aimin, Z.; Chao, L. Eur Polym J 2003, 39, 1291.
27. Zhao, D.; Liao, G.; Gao, G.; Liu, F. Macromolecules 2006, 39, 1160.
28. Naghash, H. J.; Momeni, A. R.; Alian, H.; Massah, A. R.; Ataie, S. Polym Int 2005, 54, 1564.
29. Yu, G.; Wang, J.; Liu, C.; Lin, E.; Jian, X. Polymer 2009, 50, 1700.
30. Mauritz, K. A.; Blackwell, R. I.; Beyer, F. L. Polymer 2004, 45, 3001.
31. Jose, S.; Thomas, P. S.; Thomas, S.; Karger-Kocsis, J. Polymer 2006, 47, 6328.
32. Yu, J. M.; Jerôme, R. Macromol Chem Phys 1997, 198, 3719.
33. Frey, M. W.; Cuculo, J. A.; Khan, S. A. J Polym Sci B Polym Phys 1996, 34, 2375.
34. Muller, R.; Gérard, E.; Dugand, P.; Rempp, P.; Gnanou, Y. Macromolecules 1991, 24, 1321.
35. Vega, J. F.; Muñoz, A.; Santamaria, A.; Muñoz, M. E.; Lafuente, P. Macromolecules 1996, 29, 960.
36. Ferry, J. D. Viscoelastic Properties of Polymers; Wiley: New York, 1980.
37. Shenoy, A. V.; Saini, D. R.; Nadkarni, V. M. Rheol Acta 1982, 22, 333.
38. Vargas, M. A.; Herrera, R.; Manero, O. Rubber Chem Technol 2007, 80, 340.
39. Semsarzadeh, M. A.; Barikani, S. M.; Ansari, M. Macromol Symp 2006, 239, 251.
40. Richter, S. Macromol Chem Phys 2007, 208, 1495.
41. Halász, L.; Vorster, O.; Pizzi, A.; Van Alphen, J. J Appl Polym Sci 2000, 75, 1296.
42. Jokinen, M.; Györvary, E.; Rosenholm, J. B. Colloids Surf A 1998, 141, 205.
43. Montfort, J. P.; Marin, G.; Monge, P. Macromolecules 1984, 17, 1551.
44. Aoki, Y.; Li, L.; Kakiuchi, M. Macromolecules 1998, 31, 8117.
45. Hess, W.; Vilgis, T. A.; Winter, H. H. Macromolecules 1988, 21, 2536.
46. Bhagwagar, D. E.; Serman, C. J.; Painter, P. C.; Coleman, M. M. Macromolecules 1989, 22, 4656.
47. Kojima, T.; Kurotu, T.; Kawaguchi, T. Macromolecules 1986, 19, 1284.
48. Chow, T. S. Macromol Theory Simul 1998, 7, 257.
49. Kjoniksen, A. L.; Nyström, B. Macromolecules 1996, 29, 5215.
50. Utracki, L. A. Polym Eng Sci 1988, 28, 1401.
51. Tcharkhtchi, A.; Lucas, S. A.; Trotignon, J. P.; Verdu, J. Polymer 1998, 39, 1233.
52. Kwak, S. Y.; Ahn, D. U.; Choi, J.; Song, H. J.; Lee, S. H. Polymer 2004, 45, 6889.
53. Utracki, L. A. Polym Eng Sci 1988, 28, 1401.
54. Li, Z.; Kontopoulou, M.; Polym Eng Sci 2009, 34.